PCCP

Enhancement of CO_2 adsorption on oxygen-functionalized epitaxial graphene surface at near-ambient conditions

Journal:	*Physical Chemistry Chemical Physics*
Manuscript ID	CP-ART-05-2018-003251
Article Type:	Paper
Date Submitted by the Author:	22-May-2018

Complete List of Authors:	Yamamoto, Susumu; The Institute for Solid State Physics, The University of Tokyo, Takeuchi, Kaori; The Institute for Solid State Physics, The University of Tokyo Hamamoto, Yuji; Osaka University, Department of Precision Science and Technology; Elements Strategy Initiative for Catalysts and Batteries (ESICB) Liu, Ro-ya; The Institute for Solid State Physics, The University of Tokyo; Institute of Physics, Academia Sinica Shiozawa, Yuichiro; The Institute for Solid State Physics, The University of Tokyo Koitaya, Takanori; The Institute for Solid State Physics, The University of Tokyo; The University of Tokyo, Graduate School of Arts and Sciences; Japan Science and Technology Agency (JST), Precursory Research for Embryonic Science and Technology (PRESTO) Someya, Takashi; The Institute for Solid State Physics, The University of Tokyo Tashima, Keiichiro; Tohoku University, Research Institute of Electrical Communication Fukidome, Hirokazu; Tohoku University, Research Institute of Electrical Communication Mukai, Kozo; University of Tokyo, The Institute for Solid State Physics Yoshimoto, Shinya; The Institute for Solid State Physics, The University of Tokyo Suemitsu, Maki ; Tohoku University, Research Institute of Electrical Communication, Morikawa, Yoshitada; Osaka University, Department of Precision Science and Technology, Graduate School of Engineering; Osaka University, Research Center for Ultra-Precision Science and Technology, Graduate School of Engineering Yoshinobu, Jun; University of Tokyo, The Institute for Solid State Physics Matsuda, Iwao; The Institute for Solid State Physics, The University of Tokyo

PCCP

PAPER

Enhancement of CO_2 adsorption on oxygen-functionalized epitaxial graphene surface at near-ambient conditions

Received 00th January 20xx,
Accepted 00th January 20xx

DOI: 10.1039/x0xx00000x

www.rsc.org/

Susumu Yamamoto, *[a] Kaori Takeuchi, [a] Yuji Hamamoto,[b] Ro-Ya Liu, [a, 1] Yuichiro Shiozawa, [a] Takanori Koitaya, [a, 2, 3] Takashi Someya, [a] Keiichiro Tashima, [c] Hirokazu Fukidome, [c] Kozo Mukai, [a] Shinya Yoshimoto, [a] Maki Suemitsu, [c] Yoshitada Morikawa, [b] Jun Yoshinobu [a] and Iwao Matsuda [a]

The functionalization of graphene is important in practical applications of graphene, such as in catalysts. However, the experimental study of the interactions of adsorbed molecules with functionalized graphene is difficult in ambient conditions at which catalysts are operated. Here, the adsorption of CO_2 on an oxygen-functionalized epitaxial graphene surface was studied at near-ambient conditions using ambient-pressure X-ray photoelectron spectroscopy (AP-XPS). The oxygen-functionalization of graphene is achieved *in-situ* by the photo-induced dissociation of CO_2 with X-rays on graphene in a CO_2 gas atmosphere. The oxygen species on the graphene surface is identified as the epoxy group by XPS binding energies and thermal stability. Under near-ambient conditions of 1.6 mbar CO_2 gas pressure and 175 K sample temperature, CO_2 molecules are not adsorbed on the pristine graphene, but are adsorbed on the oxygen-functionalized graphene surface. The increase in the adsorption energy of CO_2 on the oxygen-functionalized graphene surface is supported by first-principles calculations with the van der Waals density functional (vdW-DF) method. The adsorption of CO_2 on the oxygen-functionalized graphene surface is enhanced by both the electrostatic interactions between the CO_2 and the epoxy group and the vdW interactions between the CO_2 and graphene. The detailed understanding of the interaction between CO_2 and the oxygen-functionalized graphene surface obtained in this study may assist in developing guidelines for designing novel graphene-based catalysts.

1 Introduction

Graphene, a two-dimensional honeycomb lattice of carbon atoms, has great promise as a platform for catalytic reactions because it offers a high specific surface area and high electron mobility.[1-3] In catalysis applications of graphene, graphene often serves as a support material for the deposition of catalytically active metal nanoparticles.[4-6] In addition, significant efforts have been dedicated to render graphene itself catalytically active by functionalization.[7-9] For graphene functionalization, atomic species are extensively used for their simplicity: hydrogen[10, 11], fluorine[12, 13], and oxygen[14, 15] species are adsorbed on the surface of graphene and form covalent bonds with the carbon atoms. Furthermore, atomic species such as boron[16, 17] and nitrogen[16, 18] can be substitutionally incorporated into the graphene carbon network. The functionalization of graphene modifies its electronic structure, which affects the adsorptivity and chemical reactivity of molecules on graphene.

The adsorption of molecules on functionalized graphene is necessary for catalytic reactions on graphene. Despite its importance, however, experimental approaches to clarify the interactions of adsorbed molecules with functionalized graphene are limited. The experimental study of functionalized graphene surfaces at ambient conditions at which catalysts operate is particularly challenging. The recently developed method of ambient-pressure X-ray photoelectron spectroscopy (AP-XPS) permits the investigation of the electronic and chemical states of adsorbates and substrates under gas atmospheres at near-ambient pressure.[19-21]

In the present study, the adsorption of CO_2 on an oxygen-functionalized graphene surface was investigated at near-ambient conditions using AP-XPS. We present a new procedure to oxidize the graphene surface: the oxygen-functionalized graphene is prepared *in-situ* by the photo-induced dissociation of CO_2 by X-rays on graphene in a CO_2 gas atmosphere. The oxygen species on the graphene surface is identified as the epoxy group by the XPS binding energies and temperature stability. Under near-ambient conditions of 1.6 mbar CO_2 and

[a] *The Institute for Solid State Physics, The University of Tokyo, 5-1-5 Kashiwanoha, Kashiwa, Chiba 277-8581, Japan. E-mail: susumu@issp.u-tokyo.ac.jp*
[b] *Department of Precision Science and Technology, Graduate School of Engineering, Osaka University, 2-1 Yamada-oka, Suita, Osaka 565-0871, Japan.*
[c] *Research Institute of Electrical Communication, Tohoku University, 2-1-1 Katahira, Aobaku-ku, Sendai, Miyagi 980-8577, Japan.*

[1] *Present address: Institute of Physics, Academia Sinica, Nankang, Taipei 11529, Taiwan.*
[2] *Present address: Graduate School of Arts and Sciences, The University of Tokyo, 3-8-1, Komaba, Meguro-ku, Tokyo 153-8902, Japan.*
[3] *Present address: Japan Science and Technology Agency (JST), Precursory Research for Embryonic Science and Technology (PRESTO), 4-1-8 Honcho, Kawaguchi, Saitama 332-0012, Japan.*

† Electronic Supplementary Information (ESI) available: [Details of coverage calibration procedures. DFT calculations with epoxy dimers.]. See DOI: 10.1039/x0xx00000x

175 K, no CO_2 adsorption is observed on the pristine graphene, but CO_2 adsorption occurs on the oxygen-functionalized graphene surface. Thus, the oxygen-functionalization of graphene enhances the adsorption energy of CO_2. DFT calculations using the van der Waals density functional (vdW-DF) method successfully and quantitatively reproduce the increase in the adsorption energy of CO_2, simultaneously revealing the most stable adsorption site for CO_2 on the oxygen-functionalized graphene surface.

2 Experimental and theoretical methods

Well-defined monolayer epitaxial graphene on SiC(0001) was investigated in this study. The monolayer epitaxial graphene was grown on a 6H-SiC(0001) substrate by annealing at 1923 K for 1 min under Ar. The graphene was evaluated by Raman spectroscopy and low-energy electron diffraction (LEED), as reported in detail in our previous publication.[22] The graphene surface was cleaned by annealing at 773 K for 30 min in ultrahigh vacuum (UHV) conditions to remove surface contaminants adsorbed during air transfer from the graphene growth chamber to the XPS measurement chamber. The surface cleanness after the cleaning was confirmed by C 1*s* and O 1*s* XPS spectra.

The experiments were performed at the soft X-ray undulator beamline BL07LSU at SPring-8.[23] XPS measurements at near-ambient pressure were performed using an AP-XPS apparatus combining a differentially pumped electron analyzer (SPECS, PHOIBOS 150 NAP) with an ambient-pressure gas cell.[24] The cleaned graphene sample was transferred into the gas cell and exposed to near-ambient pressure CO_2 gas by filling the gas cell with CO_2. CO_2 gas (99.995% purity) was introduced into the gas cell using a mass-flow controller after reducing the amount of residual water by a cold trap. The sample temperature was monitored using a chromel-alumel (K-type) thermocouple attached to the sample surface using tantalum foil. The sample was cooled by flowing liquid N_2 in a manipulator. The incident angle of the X-ray beam and the emission angle of the photoelectrons were 68° and 0°, respectively, with respect to the surface normal. C 1*s* and O 1*s* XPS spectra were measured at the photon energy of 740 eV with a total resolution better than 600 meV. The binding energy was calibrated using the Fermi edges of Cu(110) or Cu(111) single crystals. The photon flux of soft X-rays at the sample was estimated using a photodiode (IRD AXUV-100), and by considering the transmission of the Si_3N_4 window in the gas cell and of CO_2 gas.

C 1*s* and O 1*s* XPS spectra were deconvoluted by mixed Gaussian-Lorentzian functions after a background subtraction; a Shirley background and a linear background were used for C 1*s* and O 1*s* XPS spectra, respectively. C 1*s* XPS spectra were fit with up to seven peaks: Graphene (G), SiC, surface components due to buffer layer (S1 and S2), epoxy, adsorbed CO_2 (CO_2(a)), and gas-phase CO_2 (CO_2(g)). O 1*s* XPS spectra were fit with up to four peaks: epoxy, phenol or hydroxyl (OH), CO_2(a), and CO_2(g). The details of peak fitting and the results of peak fitting parameters can be found in ESI.

The coverage of CO_2 and oxygen species on graphene is given by the fractional coverage as determined by the number of CO_2 molecules and oxygen species per surface carbon atom on the graphene (3.82×10^{15} cm^{-2} at θ = 1). The coverage calibration was performed by comparing the XPS peak intensities of CO_2 molecules and oxygen species to that of graphene in the C 1*s* XPS spectra in UHV and under near-ambient-pressure gas (see ESI).

The density functional theory (DFT) calculations were performed using the STATE code[25, 26] with norm-conserving pseudopotentials.[27] The plane-wave basis set was used with an energy cutoff of 64 Ry (400 Ry) for wave functions (charge density). The graphene surface was modeled with a periodically repeated 4 x 4 unit cell of freestanding graphene so that CO_2 coverage roughly reproduces the experimental value when a CO_2 molecule is adsorbed on the unit cell. The lattice constant of graphene was 2.46 Å and a vacuum layer of 30 Å was considered. $6 \times 6 \times 1$ *k*-points were sampled in the Brillouin zone. In order to describe the weak adsorption of CO_2 on graphene, van der Waals interactions were considered in the DFT calculations using the vdW-DF method[28] with an efficient algorithm for self-consistent calculations.[29, 30] In the vdW-DF method, we adopted the optimized Becke86b[31] exchange and the vdW-DF1 non-local correlation[28] (optB86b-vdW[32]). The optB86b-vdW functional demonstrated the greatest suitability in reproducing the adsorption energy and equilibrium distance of CO_2 on pristine graphene in our previous study.[22] The zero-point energy corrections are considered for the CO_2 molecule and the oxygen species on graphene.

3 Results and discussion

3.1 CO_2 adsorption on graphene at near ambient conditions

The adsorption of CO_2 on the pristine epitaxial graphene surface at near-ambient conditions was studied using AP-XPS. Figures 1(a) and (b) show the C 1*s* and O 1*s* XPS spectra, respectively, of the graphene surface measured under 1.6 mbar CO_2 at 175 K. The results of peak fitting are also included in the figure. The main C 1*s* peak at the binding energy (BE) of 284.7 eV is assigned to epitaxial graphene (G); the shoulder feature at 283.7 eV is ascribed to the SiC substrate (SiC).[33, 34] The peaks at 293.4 eV in the C 1*s* and 536.9 eV in the O 1*s* XPS spectra originate from gas-phase CO_2 (CO_2(g)). However, no adsorbed CO_2 molecules are observed on graphene under the present conditions.

Next the C 1*s* and O 1*s* XPS spectra of graphene were measured with increased photon flux density under the same conditions of CO_2 gas pressure and sample temperature. Figures 1(c) and (d) show the C 1*s* and O 1*s* XPS spectra of the graphene surface measured under 1.6 mbar CO_2 at 175 K with the photon flux density of 7.3×10^{16} photons/s·cm^2, which is approximately seven times higher than that used to obtain Figures 1(a) and 1(b). Unlike the AP-XPS spectra measured at the lower photon flux, new small peaks are observed at 291.2 eV in C 1*s* and at 534.7 eV in O 1*s* XPS spectra. These BEs are in good agreement with those of physisorbed CO_2 on graphene/SiC(0001) in UHV at

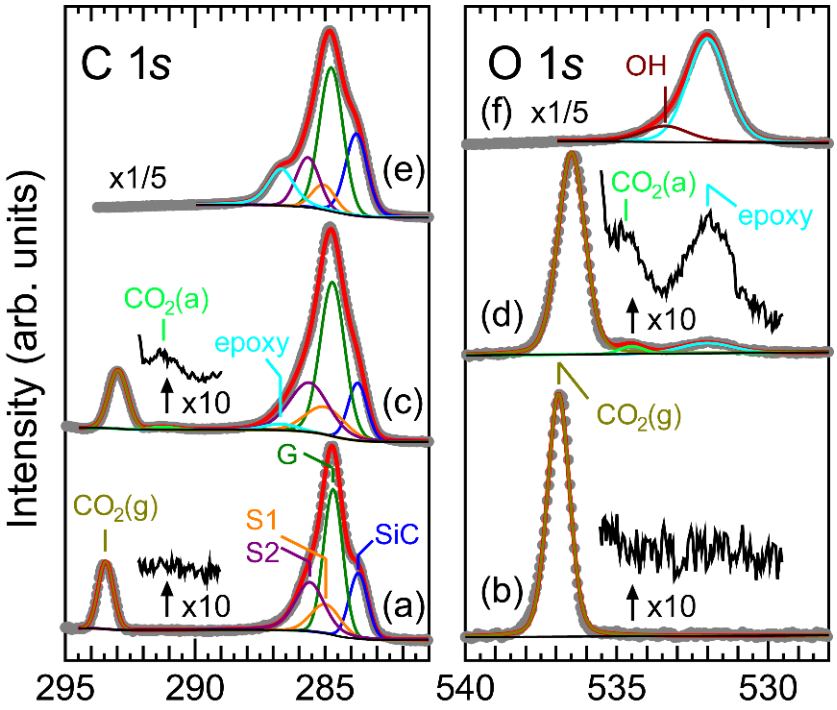

Figure 1 (a, b) C 1*s* and O 1*s* XPS spectra of the pristine epitaxial graphene measured in 1.6 mbar CO_2 at 175 K. (c, d) C 1*s* and O 1*s* XPS spectra of the oxygen-functionalized epitaxial graphene measured in 1.6 mbar CO_2 at 175 K. (e, f) C 1*s* and O 1*s* XPS spectra of the oxygen-functionalized epitaxial graphene measured in UHV at 199 K after evacuating the CO_2. The incident photon energy is 740 eV. The total energy resolution is approximately 600 meV. The photon flux densities are 1.0×10^{16} photons/s·cm^2 for (a, b), 7.3×10^{16} photons/s·cm^2 for (c, d), and 1.5×10^{16} photons/s·cm^2 for (e, f). The XPS spectra were normalized with the photon flux densities. Results of peak fitting are also included in the figure. C 1*s* XPS spectra were fit with up to seven peaks: Graphene (G), SiC, surface components due to buffer layer (S1 and S2), epoxy, adsorbed CO_2 (CO_2(a)), and gas-phase CO_2 (CO_2(g)). O 1s XPS spectra were fit with up to four peaks: epoxy, phenol or hydroxyl (OH), CO_2(a), and CO_2(g).

30 K (291.0–291.4 eV in C 1*s* and at 534.7–535.0 eV in O 1*s* XPS).[22] Therefore, the adsorption of CO_2 on graphene at near-ambient conditions can be classified as physisorption, as in UHV at 30 K. The fractional coverage of adsorbed CO_2 is estimated as 0.03. Note that the C 1*s* and O 1*s* XPS peaks of gas-phase CO_2 in Figures 1(c) and 1(d) shift to lower BE by ~0.4 eV compared to those in Figures 1(a) and 1(b). The BE shift of gas-phase peak is attributed to the change of the sample work function.[35] The origin of the sample work function change will be discussed in the next section.

Figures 1(e) and (f) show the C 1*s* and O 1*s* XPS spectra measured in UHV after evacuating CO_2 gas. After gas evacuation, neither adsorbed CO_2 nor gas-phase CO_2 are observed. Therefore, CO_2 molecules are only present on graphene under near-ambient pressure gas at 175 K.

3.2 Oxygen-functionalization of graphene

CO_2 molecules are adsorbed on the graphene only under high X-ray photon flux at near-ambient conditions. Additional XPS features are observed at 532.0 eV in O 1*s* and 286.7 eV in C 1*s* XPS spectra, as shown in Figures 1(c) and 1(d). These peak positions are in good agreement with the previously reported epoxy (C–O–C) group on graphene.[14, 36-38] The fractional coverage of the epoxy group is estimated as 0.07, larger than the coverage of CO_2 (0.03). The photo-induced dissociation of CO_2 molecules ($CO_2 \rightarrow CO + O$) at high X-ray photon flux causes the formation of epoxy groups on graphene. The oxygen-functionalized graphene surface binds CO_2 molecules more strongly than the pristine graphene surface. The sample work function change originates from the formation of epoxy groups on graphene. The generated CO is desorbed from the graphene surface at 175 K because this sample temperature is higher than the desorption temperature of the first layer CO on graphene in UHV (~48 K).[39]

In order to confirm the assignment of the oxygen species on graphene as the epoxy group, the thermal stability of the oxygen species was investigated. Figure 2 shows the C 1*s* and O 1*s* XPS spectra of the oxygen-functionalized epitaxial graphene as a function of the annealing temperature. These XPS spectra were measured in UHV after CO_2 gas evacuation. In the O 1*s* XPS spectra, the peak at 532.0 eV decreases significantly in intensity after annealing at 500 K. A concurrent intensity decrease is observed for the shoulder feature in the C 1*s* spectrum at 286.7 eV. This result is consistent with a previous report by Hossain *et al.* describing the removal of epoxy groups from graphene by annealing at 533 K.[14] The remaining O 1*s* component at ~533.4 eV after 600 K annealing could be assigned to phenol or hydroxyl (OH) groups on graphene, which were reported to survive even at a temperature of 1273 K.[40] The OH groups were also observed on graphene in Figure 1 (f) after CO_2 gas evacuation at 175 K. The OH groups are most likely formed by photo-induced reactions and/or thermal reactions of epoxy oxygen with either small amount of residual H_2O in near-ambient pressure CO_2 vapor or hydrocarbon (C_xH_y) species that

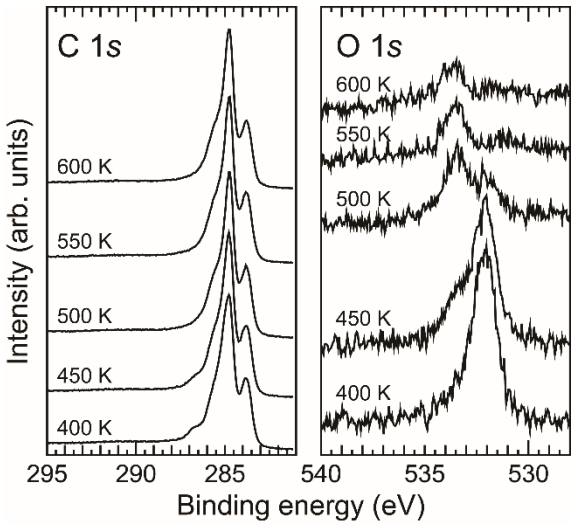

Figure 2 C 1*s* and O 1*s* XPS spectra of the oxygen-functionalized epitaxial graphene as functions of annealing temperature. XPS spectra are measured in UHV after CO_2 gas evacuation. The incident photon energy is 740 eV. The total energy resolution is approximately 220 meV.

are present on the inner wall of gas cell and displaced by CO_2 molecules at near-ambient pressures. As discussed above, the thermal stability of the oxygen species also supports the identification of the oxygen species as epoxy groups.

Here the oxygen-functionalized graphene was prepared *in-situ* by the photo-induced dissociation of CO_2 by X-ray beams on graphene in CO_2 gas. Several methods can be used to produce oxygen-functionalized graphene: (1) solution-phase oxidation (*e.g.*, Hummers' method),[41-43] (2) atomic oxygen exposure,[14, 38, 44-47] (3) e-beam irradiation in air,[48, 49] (4) ultraviolet (UV)/O_3 treatment,[50] and (5) the photo-induced dissociation of oxygen-containing molecules.[36, 37] The oxidation procedure of graphene used here is part of category (5). In previous studies, oxygen-containing molecules (NO_2[36] or SO_2[37]) were adsorbed on graphene at 100 K in UHV, and then exposed to X-rays. The photo-induced dissociation of NO_2 or SO_2 caused the formation of epoxy groups on the graphene.[36, 37] The photon flux density in these previous studies was approximately 10^{18} photons/s·cm^2, somewhat higher than that in this study (7.3×10^{16} photons/s·cm^2). We thus report the first oxygen-functionalization of graphene by the photo-induced dissociation of oxygen-containing molecules under a more realistic condition of near-ambient-pressure gas.

3.3 DFT calculation

In order to understand the interactions between the oxygen-functionalized graphene surface and the CO_2 molecules, DFT calculations were performed using the vdW-DF method. Although the structural and electronic properties of epoxy groups on graphene have been studied extensively using DFT calculations,[14, 15, 51-65] theoretical investigations on the interactions of adsorbed molecules with epoxy groups on graphene remain limited.

Figure 3 (a) shows the structural model used in the DFT calculations. A single epoxy oxygen atom is adsorbed in the 4 × 4 unit cell of freestanding graphene. We confirmed that the CO_2 adsorption energy on the pristine graphene does not significantly depend on the adsorption site or the in-plane orientation. Thus only three different positions are investigated as the adsorption sites for the CO_2 molecule on the oxygen-functionalized graphene, as indicated in Figure 3 (a). Bird's-eye view of a CO_2 molecule adsorbed at position 2 on the oxygen-functionalized graphene is shown in Figure 3 (b). The orientation of the CO_2 molecule is set as parallel to the C–C bond of graphene. The coverage of the epoxy group and CO_2 molecules in this structural model is 0.031. The coverage of CO_2 molecules in the DFT calculations thus matches that observed in the experiment (0.03). The interaction energy, E_{int}, between CO_2 and the oxygen-functionalized graphene is defined as $E_{\mathrm{int}} = E_{\mathrm{CO_2/O-Gra}} - E_{\mathrm{CO_2}} - E_{\mathrm{O-Gra}}$, where $E_{\mathrm{CO_2}}$, $E_{\mathrm{O-Gra}}$, and $E_{\mathrm{CO_2/O-Gra}}$ are the total energies of an isolated CO_2 molecule, oxygen-functionalized graphene, and the adsorbed system, respectively.

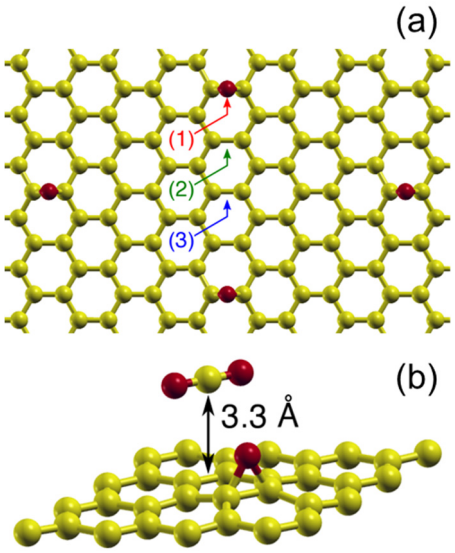

Figure 3 (a) The structural model of CO_2 adsorbed on the oxygen-functionalized graphene. The oxygen species on graphene is an epoxy (C–O–C) group. The epoxy group and CO_2 molecules are adsorbed in the 4 × 4 unit cell of freestanding graphene (θ = 0.031). Three different positions are considered as the adsorption sites for the CO_2 molecule on the oxygen-functionalized graphene. (b) bird's-eye view of a CO_2 molecule adsorbed at position (2) on the oxygen-functionalized graphene.

In Figure 4, the interaction energies of CO_2 on the pristine and oxygen-functionalized graphene surfaces are calculated as a function of distance between the CO_2 and graphene with the geometries fixed to the reference systems. By fully relaxing the geometries near the minima, the interaction energies at the equilibrium distance d_{eq} are obtained. On the pristine graphene surface, $|E_{int}|$ of CO_2 is 20.2 (19.2) kJ/mol at d_{eq} = 3.29 Å without (with) the zero-point energy corrections. $|E_{int}|$ of CO_2 on graphene was reported as 24.7 (23.5) kJ/mol in our previous publication[22] for CO_2 molecules in a 2 × 2 unit cell (θ = 0.125). The difference in $|E_{int}|$ of CO_2 on graphene originates from the difference in the unit cell size. For larger unit cells or lower coverage, the intermolecular attraction between CO_2 molecules diminishes, thereby decreasing $|E_{int}|$. This is demonstrated by

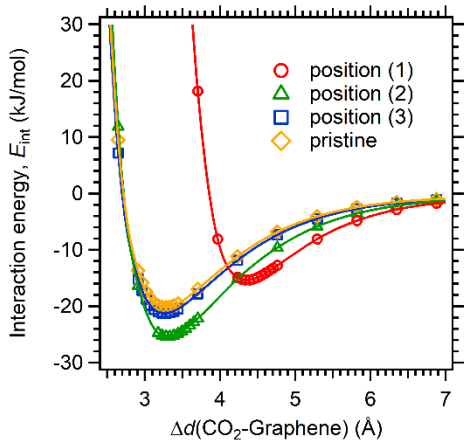

Figure 4 Interaction energy as a function of distance Δ*d* between CO_2 and graphene. For comparison, the interaction energy of CO_2 on the pristine graphene surface is calculated and shown. The DFT calculations are performed with the optB86b-vdW functional.

the interaction energy at large distance approaching zero, as seen in Figure 4.

Now we compare the adsorption energies of CO_2 on the oxygen-functionalized graphene surface at the three different adsorption sites shown in Figure 3 (a). First, we review position 1, at which a CO_2 molecule is adsorbed on top of the epoxy group. $|E_{int}|$ of CO_2 is as small as 15.6 (14.1) kJ/mol at d_{eq}= 4.36 Å. At position 1, the CO_2 molecule is insufficiently stabilized by the vdW attraction from graphene because Pauli repulsion from the epoxy group prevents the CO_2 molecule from approaching the graphene. Next, we consider position 2, at which the CO_2 molecule is adsorbed on the C–C bond of graphene next to the epoxy group. $|E_{int}|$ of CO_2 is 25.7 (24.5) kJ/mol at d_{eq}= 3.32 Å. Compared to $|E_{int}|$ of CO_2 on the pristine graphene surface (20.2 kJ/mol), $|E_{int}|$ of CO_2 increases by ~5 kJ/mol on the oxygen-functionalized graphene surface. At position 2, the interaction energy is increased by both the electrostatic interaction between the CO_2 and epoxy group and the vdW interaction between the CO_2 and graphene. Finally, we consider position 3, at which the CO_2 molecule is adsorbed on the C–C bond of graphene farther from the epoxy group. $|E_{int}|$ of CO_2 is 21.5 (20.4) kJ/mol at d_{eq} = 3.27 Å, similar to the value on the pristine graphene surface (*i.e.*, 20.2 kJ/mol at d_{eq} = 3.29 Å). This is explained by the disappearance of electrostatic interactions between the CO_2 and epoxy group because of the distance between the two.

To summarize the above, the interaction energy of CO_2 on the oxygen-functionalized graphene surface is higher by ~5 kJ/mol than that on the pristine graphene surface. The most stable adsorption site of CO_2 among the three sites investigated here is the C–C bond next to the epoxy group (position 2). This is because the adsorption of CO_2 is stabilized by both the electrostatic interactions between the CO_2 and epoxy group and the vdW interactions between the CO_2 and graphene. While the coverage of the epoxy groups used for the calculations is approximately half that of the experimental estimation, the behavior of CO_2 adsorption on the oxygen-functionalized graphene is essentially unchanged at higher coverage (see ESI).

3.4 Discussion

In ambient-pressure XPS experiments, an equilibrium exists between adsorption and desorption; the rate of adsorption is equal to the rate of desorption. The rate of adsorption r_{ads} is expressed as the product of the incident molecular flux *F* and sticking probability *s*:

$$r_{ads} = F \cdot s = \frac{p}{\sqrt{2\pi mkT}} \cdot s \qquad (1)$$

where *p* is the gas pressure, *m* the molecular mass, and *T* the gas temperature.

The rate of desorption r_{des} is expressed as follows:

$$r_{des} = \nu_{des} \cdot exp\left(-\frac{E_{des}}{RT}\right) \cdot \theta^n \qquad (2)$$

where ν_{des} is the pre-exponential factor for desorption, E_{des} the desorption energy, *R* the gas constant, *T* the sample temperature, θ the coverage of adsorbed molecules, and *n* the desorption order.

Under the equilibrium condition (r_{ads} = r_{des}), the change in desorption energy ΔE_{des} of CO_2 on graphene by epoxy formation can be derived by the following equation:

$$\Delta E_{des} = -RT \ln\left(\theta/\theta' \cdot s'/s\right) \qquad (3)$$

where θ (*s*) and θ'(*s*′) are the coverage (sticking probability) of CO_2 without and with epoxy groups, respectively. Here we assume first-order desorption kinetics (*n* = 1) and that the pre-exponential factor for desorption remains constant with epoxy formation (*i.e.*, ν_{des} = ν_{des}').

In the AP-XPS spectra, no adsorbed CO_2 molecules are observed on the pristine graphene surface without epoxy groups. The coverage of CO_2 θ is below the detection limit of 0.001. The coverage of CO_2 after epoxy formation, θ', is 0.03. Since the change in sticking probability by epoxy formation is not experimentally determined, *s*′/*s* is assumed to be unity. By inserting these numbers ($\theta \leq$ 0.001, θ' = 0.03, and *s*′/*s* = 1) into Eq. (3), the increase in CO_2 desorption energy ΔE_{des} by epoxy formation is calculated as ≥ 5.0 kJ/mol: $\Delta E_{des} \geq$ 5.0 kJ/mol. Therefore, the experimentally derived increase in desorption (adsorption) energy of CO_2 on the oxygen-functionalized graphene is in good agreement with that obtained by the DFT calculations.

Conclusions

The adsorption of CO_2 on the oxygen-functionalized graphene surface was studied at near-ambient conditions using AP-XPS. The oxygen functionalization of the monolayer epitaxial graphene on SiC(0001) was achieved *in-situ* by the photo-induced dissociation of CO_2 with X-rays. The oxygen species on the graphene surface was identified as the epoxy group based on the XPS binding energy and thermal stability. Under near-ambient conditions of 1.6 mbar CO_2 gas pressure and 175 K sample temperature, no CO_2 adsorption was observed on the pristine graphene, but CO_2 adsorption occurred on the oxygen-functionalized graphene surface. The increase in CO_2 adsorption energy by epoxy formation was determined as ≥5.0 kJ/mol from the adsorption and desorption equilibrium relationship. This increase was successfully reproduced by DFT calculations with the vdW-DF method. In addition, DFT calculations revealed that

the most stable adsorption site of CO_2 on the oxygen-functionalized graphene surface is not on top of the epoxy group, but on the C–C bond of graphene adjacent to the epoxy group. The adsorption of CO_2 on the oxygen-functionalized graphene surface is stabilized by both the electrostatic interactions between the CO_2 and epoxy group and the vdW interactions between the CO_2 and graphene.

Conflicts of interest

There are no conflicts to declare.

Acknowledgements

The present work was supported by the Advanced-Catalytic-Transformation Program for Carbon Utilization (ACT-C) of the Japan Science and Technology Agency (JST) (Grant No. JPMJCR12YU), the Grand-in Aid for Scientific Research on Innovative Area “3D Active-Site Science”, and the Grant-in-Aid for Young Scientists (A) (No. 16H06027) from the Japanese Society for the Promotion of Sciences (JSPS). The experiment was carried out as joint research in the Synchrotron Radiation Research Organization and The Institute for Solid State Physics, The University of Tokyo (Proposal No. 2015A7490, 2015B7496, 2016A7401, 2016B7401, 2017A7401, and 2017B7401). K.T. acknowledges financial support from the Ministry of Education, Culture, Sports, Science and Technology of Japan (Photon and Quantum Basic Research Coordinated Development Program). R.L. acknowledges financial support from The University of Tokyo Fellowship, Special Scholarship Program for International Students. Y.S. acknowledges financial support from The University of Tokyo, Research Assistantship Program.

References

1. A. K. Geim, *Science*, 2009, **324**, 1530-1534.
2. K. S. Novoselov, V. I. Fal'ko, L. Colombo, P. R. Gellert, M. G. Schwab and K. Kim, *Nature*, 2012, **490**, 192-200.
3. A. C. Ferrari, F. Bonaccorso, V. Fal'ko, K. S. Novoselov, S. Roche, P. Boggild, S. Borini, F. H. L. Koppens, V. Palermo, N. Pugno, J. A. Garrido, R. Sordan, A. Bianco, L. Ballerini, M. Prato, E. Lidorikis, J. Kivioja, C. Marinelli, T. Ryhanen, A. Morpurgo, J. N. Coleman, V. Nicolosi, L. Colombo, A. Fert, M. Garcia-Hernandez, A. Bachtold, G. F. Schneider, F. Guinea, C. Dekker, M. Barbone, Z. Sun, C. Galiotis, A. N. Grigorenko, G. Konstantatos, A. Kis, M. Katsnelson, L. Vandersypen, A. Loiseau, V. Morandi, D. Neumaier, E. Treossi, V. Pellegrini, M. Polini, A. Tredicucci, G. M. Williams, B. Hee Hong, J.-H. Ahn, J. Min Kim, H. Zirath, B. J. van Wees, H. van der Zant, L. Occhipinti, A. Di Matteo, I. A. Kinloch, T. Seyller, E. Quesnel, X. Feng, K. Teo, N. Rupesinghe, P. Hakonen, S. R. T. Neil, Q. Tannock, T. Lofwander and J. Kinaret, *Nanoscale*, 2015, **7**, 4598-4810.
4. E. Yoo, T. Okata, T. Akita, M. Kohyama, J. Nakamura and I. Honma, *Nano Lett.*, 2009, **9**, 2255-2259.
5. P. V. Kamat, *J. Phys. Chem. Lett.*, 2010, **1**, 520-527.
6. N. M. Julkapli and S. Bagheri, *Int. J. Hydrogen Energy*, 2015, **40**, 948-979.
7. D.-e. Jiang and Z. Chen, *Graphene chemistry : theoretical perspectives*, John Wiley & Sons, Chichester, West Sussex, 2013.
8. J. E. Johns and M. C. Hersam, *Acc. Chem. Res.*, 2013, **46**, 77-86.
9. U. N. Maiti, W. J. Lee, J. M. Lee, Y. Oh, J. Y. Kim, J. E. Kim, J. Shim, T. H. Han and S. O. Kim, *Adv. Mater.*, 2014, **26**, 40-67.
10. D. C. Elias, R. R. Nair, T. M. G. Mohiuddin, S. V. Morozov, P. Blake, M. P. Halsall, A. C. Ferrari, D. W. Boukhvalov, M. I. Katsnelson, A. K. Geim and K. S. Novoselov, *Science*, 2009, **323**, 610-613.
11. S. Rajasekaran, F. Abild-Pedersen, H. Ogasawara, A. Nilsson and S. Kaya, *Phys. Rev. Lett.*, 2013, **111**, 085503.
12. R. R. Nair, W. Ren, R. Jalil, I. Riaz, V. G. Kravets, L. Britnell, P. Blake, F. Schedin, A. S. Mayorov, S. Yuan, M. I. Katsnelson, H.-M. Cheng, W. Strupinski, L. G. Bulusheva, A. V. Okotrub, I. V. Grigorieva, A. N. Grigorenko, K. S. Novoselov and A. K. Geim, *Small*, 2010, **6**, 2877-2884.
13. R. Zbořil, F. Karlický, A. B. Bourlinos, T. A. Steriotis, A. K. Stubos, V. Georgakilas, K. Šafářová, D. Jančík, C. Trapalis and M. Otyepka, *Small*, 2010, **6**, 2885-2891.
14. M. Z. Hossain, J. E. Johns, K. H. Bevan, H. J. Karmel, Y. T. Liang, S. Yoshimoto, K. Mukai, T. Koitaya, J. Yoshinobu, M. Kawai, A. M. Lear, L. L. Kesmodel, S. L. Tait and M. C. Hersam, *Nature Chemistry*, 2012, **4**, 305-309.
15. J. Jung, H. Lim, J. Oh and Y. Kim, *J. Am. Chem. Soc.*, 2014, **136**, 8528-8531.
16. L. S. Panchakarla, K. S. Subrahmanyam, S. K. Saha, A. Govindaraj, H. R. Krishnamurthy, U. V. Waghmare and C. N. R. Rao, *Adv. Mater.*, 2009, **21**, 4726-4730.
17. L. Zhao, M. Levendorf, S. Goncher, T. Schiros, L. Pálová, A. Zabet-Khosousi, K. T. Rim, C. Gutiérrez, D. Nordlund, C. Jaye, M. Hybertsen, D. Reichman, G. W. Flynn, J. Park and A. N. Pasupathy, *Nano Lett.*, 2013, **13**, 4659-4665.
18. D. Guo, R. Shibuya, C. Akiba, S. Saji, T. Kondo and J. Nakamura, *Science*, 2016, **351**, 361-365.
19. M. Salmeron and R. Schlögl, *Surf. Sci. Rep.*, 2008, **63**, 169-199.
20. D. E. Starr, Z. Liu, M. Hävecker, A. Knop-Gericke and H. Bluhm, *Chem. Soc. Rev.*, 2013, **42**, 5833-5857.
21. S. Yamamoto, H. Bluhm, K. Andersson, G. Ketteler, H. Ogasawara, M. Salmeron and A. Nilsson, *J. Phys.: Condens. Matter*, 2008, **20**, 184025.
22. K. Takeuchi, S. Yamamoto, Y. Hamamoto, Y. Shiozawa, K. Tashima, H. Fukidome, T. Koitaya, K. Mukai, S. Yoshimoto, M. Suemitsu, Y. Morikawa, J. Yoshinobu and I. Matsuda, *J. Phys. Chem. C*, 2017, **121**, 2807-2814.
23. S. Yamamoto, Y. Senba, T. Tanaka, H. Ohashi, T. Hirono, H. Kimura, M. Fujisawa, J. Miyawaki, A. Harasawa, T. Seike, S. Takahashi, N. Nariyama, T. Matsushita, M. Takeuchi, T. Ohata, Y. Furukawa, K. Takeshita, S. Goto, Y. Harada, S. Shin, H. Kitamura, A. Kakizaki, M. Oshima and I. Matsuda, *J. Synchrotron Rad.*, 2014, **21**, 352-365.
24. T. Koitaya, S. Yamamoto, Y. Shiozawa, K. Takeuchi, R.-Y. Liu, K. Mukai, S. Yoshimoto, K. Akikubo, I. Matsuda and J. Yoshinobu, *Top. Catal.*, 2016, **59**, 526-531.
25. Y. Morikawa, K. Iwata and K. Terakura, *Appl. Surf. Sci.*, 2001, **169–170**, 11-15.
26. Y. Hamamoto, I. Hamada, K. Inagaki and Y. Morikawa, *Phys. Rev. B*, 2016, **93**, 245440.

27. N. Troullier and J. L. Martins, *Phys. Rev. B*, 1991, **43**, 1993-2006.
28. M. Dion, H. Rydberg, E. Schröder, D. C. Langreth and B. I. Lundqvist, *Phys. Rev. Lett.*, 2004, **92**, 246401.
29. G. Román-Pérez and J. M. Soler, *Phys. Rev. Lett.*, 2009, **103**, 096102.
30. J. Wu and F. Gygi, *J. Chem. Phys.*, 2012, **136**, 224107.
31. A. D. Becke, *J. Chem. Phys.*, 1986, **85**, 7184-7187.
32. J. Klimeš, D. R. Bowler and A. Michaelides, *Phys. Rev. B*, 2011, **83**, 195131.
33. K. V. Emtsev, A. Bostwick, K. Horn, J. Jobst, G. L. Kellogg, L. Ley, J. L. McChesney, T. Ohta, S. A. Reshanov, J. Rohrl, E. Rotenberg, A. K. Schmid, D. Waldmann, H. B. Weber and T. Seyller, *Nat Mater*, 2009, **8**, 203-207.
34. C. Riedl, C. Coletti and U. Starke, *J. Phys. D: Appl. Phys.*, 2010, **43**, 374009.
35. S. Axnanda, M. Scheele, E. Crumlin, B. Mao, R. Chang, S. Rani, M. Faiz, S. Wang, A. P. Alivisatos and Z. Liu, *Nano Lett.*, 2013, **13**, 6176-6182.
36. S. Böttcher, H. Vita and K. Horn, *Surf. Sci.*, 2014, **621**, 117-122.
37. S. Böttcher, H. Vita and K. Horn, *Surf. Sci.*, 2015, **641**, 305-309.
38. E. Velez-Fort, A. Ouerghi, M. G. Silly, M. Eddrief, A. Shukla, F. Sirtti and M. Marangolo, *Appl. Phys. Lett.*, 2014, **104**, 4.
39. R. S. Smith, R. A. May and B. D. Kay, *J. Phys. Chem. B*, 2016, **120**, 1979-1987.
40. A. Ganguly, S. Sharma, P. Papakonstantinou and J. Hamilton, *J. Phys. Chem. C*, 2011, **115**, 17009-17019.
41. W. S. Hummers and R. E. Offeman, *J. Am. Chem. Soc.*, 1958, **80**, 1339-1339.
42. D. C. Marcano, D. V. Kosynkin, J. M. Berlin, A. Sinitskii, Z. Sun, A. Slesarev, L. B. Alemany, W. Lu and J. M. Tour, *ACS Nano*, 2010, **4**, 4806-4814.
43. M. Z. Hossain, M. B. A. Razak, S. Yoshimoto, K. Mukai, T. Koitaya, J. Yoshinobu, H. Sone, S. Hosaka and M. C. Hersam, *J. Phys. Chem. C*, 2014, **118**, 1014-1020.
44. N. A. Vinogradov, K. Schulte, M. L. Ng, A. Mikkelsen, E. Lundgren, N. Martensson and A. B. Preobrajenski, *J. Phys. Chem. C*, 2011, **115**, 9568-9577.
45. R. Larciprete, S. Fabris, T. Sun, P. Lacovig, A. Baraldi and S. Lizzit, *J. Am. Chem. Soc.*, 2011, **133**, 17315-17321.
46. T. Takahashi, K. Sugawara, E. Noguchi, T. Sato and T. Takahashi, *Carbon*, 2014, **73**, 141-145.
47. A. J. Marsden, P. Brommer, J. J. Mudd, M. A. Dyson, R. Cook, M. Asensio, J. Avila, A. Levy, J. Sloan, D. Quigley, G. R. Bell and N. R. Wilson, *Nano Research*, 2015, **8**, 2620-2635.
48. K.-j. Kim, J. Choi, H. Lee, H.-K. Lee, T.-H. Kang, Y.-H. Han, B.-C. Lee, S. Kim and B. Kim, *J. Phys. Chem. C*, 2008, **112**, 13062-13064.
49. Z. Xu, L. Chen, J. Li, R. Wang, X. Qian, X. Song, L. Liu and G. Chen, *Appl. Phys. Lett.*, 2011, **98**, 183112.
50. Y. Mulyana, M. Uenuma, Y. Ishikawa and Y. Uraoka, *J. Phys. Chem. C*, 2014, **118**, 27372-27381.
51. D. C. Sorescu, K. D. Jordan and P. Avouris, *J. Phys. Chem. B*, 2001, **105**, 11227-11232.
52. J.-L. Li, K. N. Kudin, M. J. McAllister, R. K. Prud'homme, I. A. Aksay and R. Car, *Phys. Rev. Lett.*, 2006, **96**, 176101.
53. D. W. Boukhvalov and M. I. Katsnelson, *J. Am. Chem. Soc.*, 2008, **130**, 10697-10701.
54. R. J. W. E. Lahaye, H. K. Jeong, C. Y. Park and Y. H. Lee, *Phys. Rev. B*, 2009, **79**, 125435.
55. Z. Li, W. Zhang, Y. Luo, J. Yang and J. G. Hou, *J. Am. Chem. Soc.*, 2009, **131**, 6320-6321.
56. J.-A. Yan, L. Xian and M. Y. Chou, *Phys. Rev. Lett.*, 2009, **103**, 086802.
57. L. Wang, Y. Y. Sun, K. Lee, D. West, Z. F. Chen, J. J. Zhao and S. B. Zhang, *Phys. Rev. B*, 2010, **82**, 161406.
58. H. J. Xiang, S.-H. Wei and X. G. Gong, *Phys. Rev. B*, 2010, **82**, 035416.
59. J.-A. Yan and M. Y. Chou, *Phys. Rev. B*, 2010, **82**, 125403.
60. N. Lu, D. Yin, Z. Li and J. Yang, *J. Phys. Chem. C*, 2011, **115**, 11991-11995.
61. D. K. Samarakoon and X.-Q. Wang, *Nanoscale*, 2011, **3**, 192-195.
62. S. Tang and Z. Cao, *J. Chem. Phys.*, 2011, **134**, 044710.
63. M. Topsakal and S. Ciraci, *Phys. Rev. B*, 2012, **86**, 205402.
64. S. Tang and Z. Cao, *J. Phys. Chem. C*, 2012, **116**, 8778-8791.
65. Ž. Šljivančanin, A. S. Milošević, Z. S. Popović and F. R. Vukajlović, *Carbon*, 2013, **54**, 482-488.

Table of contents entry

Enhancement of CO_2 adsorption on the functionalized graphene with epoxy oxygen was found by ambient-pressure XPS. The origin of the increased interaction energy was revealed by DFT calculations that include vdW interactions.